Defence Science Journal, Vol. 63, No. 6, November 2013, pp. 571-580, DOI : 10.14429/dsj.63.5756

Development of Miniature Stirling Cryocooler Technology for Infrared Focal Plane Array

Manmohan Singh*, Mukesh Sadana, Sunil Sachdev, and Gaurav Pratap
Solid State Physics Laboratory, Delhi-110 054, India
**E-mail: manmohan.f@sspl.drdo.in*

ABSTRACT

A reliable miniature cryocooler is one of the basic and foremost requirements for successful operation of high performance cooled infrared focal plane array (IRFPA) used for defence applications. Technological complexity and requirement of long duration fail-safe operation of the cryocooler demands robust design, fabrication and assembly with tolerances and, perfection of an array of sub-technologies. The paper presents the progress of the development activities in Stirling cryocooler technology at Solid State Physics Laboratory (SSPL), which evolved through essential milestones like the development of single and dual piston linear motor driven split coolers to the state-of-the-art integral Brushless DC (BLDC) motor crank-driven type highly miniaturized coolers of capacities ranging from 0.25 to 0.5W at 80K. The theoretical investigations in the design of Stirling cycle cryocooler have been reported and the issues related to the design aspects are discussed in sufficient details. Experimental results of cryocooler performance tests are also presented. The paper also focuses on regenerator design optimization. The results of optimizations have been shown at the end considering a sample data.

Keywords: Cryocooler, stirling, regenerator, infrared, infrared focal plane array

NOMENCLATURE

A_f	Mean sectional area of void space
A_r	Area of regenerator cross-section
A_t	Regenerator tube cross-sectional area
C_m	Specific heat of matrix material
d_m	Mesh wire diameter
d_r	Internal diameter of regenerator tube
h_m	Mean heat transfer coefficient
k	Thermal conductivity
l	Length
l_m	Mesh distance
M	Mass of matrix
n	No. of wire mesh screens
N_{TOTAL}	Total of different mesh size considered
r	Compression ratio
T	Temperature
t	Blow time
u	Velocity of fluid in matrix
ρ	Density
υ	Kinematic viscosity
Subscripts	
m	of matrix
f	of fluid
r	Regenerator
0	Void space
c	Compression
e	Expansion

1. INTRODUCTION

Currently a large number of infrared (IR) detectors for night vision devices and missile guidance systems are in use. The temperature needed for cooling these detectors are, for the most part, lower than those produced by conventional refrigeration, and lies in cryogenic range[1,2,3]. These systems need miniature cryocooler of 0.25 W to 1 W at 80 K capacity for their cooling requirements. To meet this requirement various types of cryocoolers such as Stirling, Joule-Thomson and others have been investigated in the past few decades[4]. Stirling cryocoolers have emerged as preferred systems in terms of efficiency, low mass, compactness and relatively low production cost in the capacity ranges of interest. Various forms of Stirling cryocoolers e.g. split linear motor driven, integral rotary crank driven etc. having capacities of less than a Watt are already being manufactured by various companies across the world. Pioneer work was done by Stolfi[5] in the development of miniature free piston free displacer (FPFD) cryocooler with a capacity of 1 W at 77 K. This cooler utilizes linear electric drive, resulting in long life cryocooler as there was no wear and tear caused by side forces. A detailed theoretical analysis is also given by Dejong[6] and Koh[7]. The basic thermodynamic analysis of stirling cycle was attempted by walker[8], and later Tailor[9] presented it considering the dead volume and imperfect regeneration effects. A lot of work has been reported on the loss analysis of cryocooler. Orlowska[10] has reported measurement of all the significant losses, whereas Reed[11] and Yang[12] analyzed the system losses related to compressor and expander subsystems respectively.

The SSPL is working in the field of IRFPA detectors for quite some time. As a part of this activity for cooling needs of the detector array, development of stirling cryocoolers has assumed the main focus apart from Joule-Thomson (JT) coolers for certain night vision equipment applications. In the

Received 17 September 2013, online published 18 December 2013

past SSPL has worked on development of linear motor driven integral[13] and split FPFD cryocoolers in single and dual piston configurations. Over the period of time, the focus has shifted gradually towards developing integrated cooler of crank driven type owing to its advantages especially suited to night vision equipment over the split configurations.

In this paper, a brief of activities starting from the theoretical background to the prototype development, covering mostly the related theoretical as well as practical design aspects has been discussed. The losses which are the main governing element in deciding the configuration and design are discussed. An attempt has also been made in optimizing the design of regenerative heat exchanger, called regenerator.

2. LINEAR MOTOR DRIVEN SPLIT CRYOCOOLER

Miniature split cryocoolers, in both single and dual piston FPFD configurations having capacities 0.25 W to 0.5 W at 80 K have been developed at SSPL for ground based applications. In earlier cooler design with single piston[14], the gas was compressed by axial movement of piston generating an axial thrust due to inherent high inertia, which in turn generates high vibrations and EM noise in cold region. This necessitated a passive vibration absorber in which a floating mass acts as a damper. This arrangement too was not able to completely eliminate the vibrations due to less predictable behaviour of the movement of free piston. The absorber increased not only the weight and size of the system but also the complexity due to more running components, thereby rendering this a low reliability system. To overcome these shortcomings of the single piston system, dual piston system was introduced in which the compressor was provided with two linear motors driving two co-axial pistons positioned 180° out of phase against a common compression volume, thereby mutually balancing the axial thrust and eliminating the related vibrations. Prototype of the dual piston cryocooler is shown in Fig. 1(a).

2.1 Results

The prototype was tested for its performance using dummy vacuum jacket around the cold tip with a vacuum of the order of 10^{-5} millibar. Heat load was externally applied using a resistive heater element and cold tip temperature was monitored using a PT-100 RTD. Experimental results are shown in Fig. 1(b). The cold-tip temperature well below the required 80 K mark achieved at no-load conditions is shown in Fig. 1(b) which was obtained during a typical 100 h test.

3. INTEGRAL CRANK DRIVEN CRYOCOOLER

As the work on the development of 320 x 256 MW IRFPA progressed at SSPL, requirement changed to smaller, compact and high efficiency cryocoolers. Therefore, the focus was shifted to the development of rotary integral cryocoolers. Earlier the rotary coolers were using dry rubbing seals which were a limiting factor in terms of reliability and lifetime as compared to linear motor cryocoolers. Later, with the advancement in manufacturing technology, rubbing seals were replaced by dynamic clearance seals, making the rotary coolers comparable to the linear motor systems in terms of lifetime and reliability. The integrated detector/dewar cooler assembly (IDCA) configuration was chosen owing to a number of advantages offered by this over linear motor coolers. The relevant system description and developmental work is presented in the following sections.

3.1 System Description

The schematic of IDCA cryocooler assembly is shown in Figure 2. The cryocooler system is complex assembly of mechanical parts in which the compressor and expander modules are connected by a small internal delivery duct which is drilled inside the body of the cryocooler. The cooler is charged with high purity Helium gas which is used as refrigerant. The compression is achieved inside the piston- cylinder assembly in which the piston moves at a frequency in the range of 50

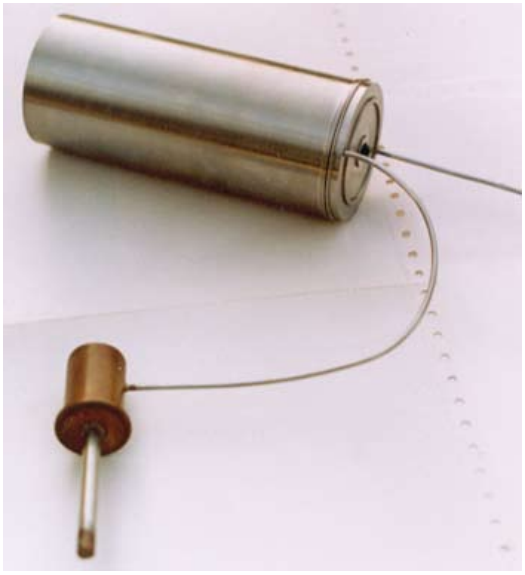

(a)

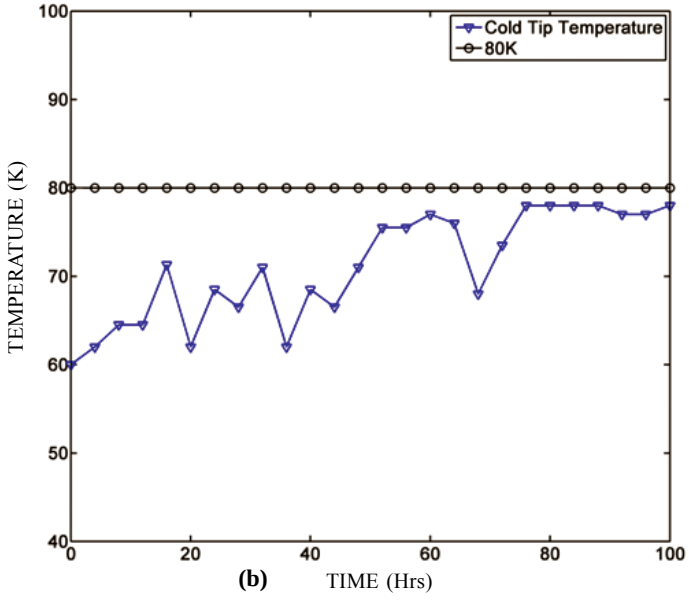

(b)

Figure 1. (a) Linear motor driven dual piston split cryocooler prototype of capacity 0.5W@80K (b) Cold-tip temperature during long performance run with Input power of 32 W.

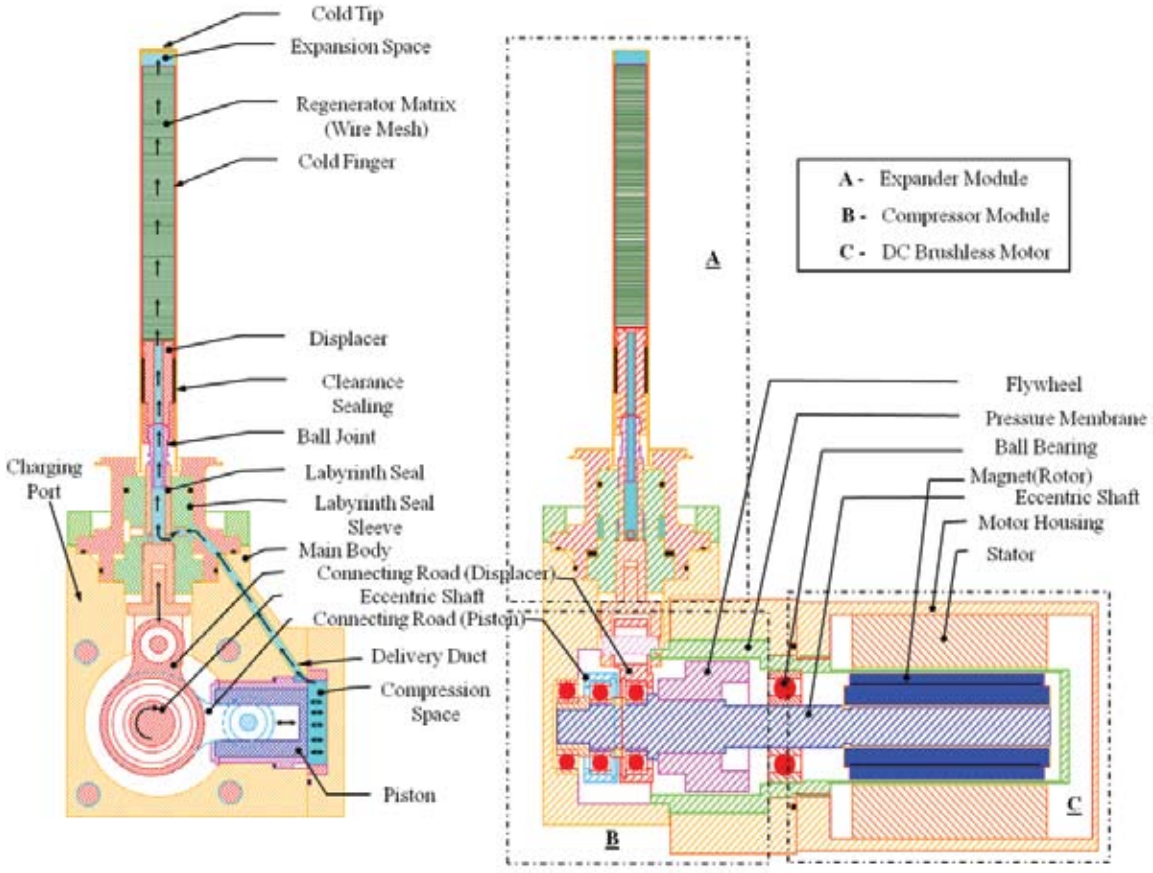

Figure 2. Schematic assembly view of IDCA cryocooler.

to 75 Hz. The cold-finger cylinder in which the expansion takes place is attached to the crankcase and is placed at right angle to the compressor cylinder to ensure an optimum phase relationship. The drive mechanism used is of slider-crank type, in which there are two separate connecting rods attached to a single crank-shaft, called the eccentric shaft, and drive is provided by a BLDC motor[16].

The displacer cum regenerator consists of a fiber glass epoxy tube stacked with a number of SS wire-mesh discs. A flywheel made of high density special sintered alloy has been used for regulating the motor torque. Dynamic balancing of unbalance rotary masses has been done using the flywheel itself as a balance mass because of space constraints. The ground link of mechanism i.e. the main body is made up of special Aluminum alloy for added strength apart from fulfilling the high thermal conductivity and machinability requirements.

Dynamic clearance seals with precisely controlled geometry and surface finishes have been used for guiding the displacer and piston in their respective pair for preventing the occurrence of wear by rubbing, and hence negates the need for lubrication. An experimentally optimized radial clearance value of 7 µm - 8 µm is found to be the perfect enough for piston-cylinder arrangement. To achieve this sort of clearances, manufacturing process was developed to fabricate the seals and bearings in close tolerances. The piston-cylinder pair is lapped and polished to the surface finishes of the order of 0.05 µm Ra, and the piston is coated with a very high hardness special ceramic material with a low coefficient of friction to reduce wear. Further, the motor winding has been kept out of Helium atmosphere with the use of thin cylinder, called the pressure membrane, for keeping the cooler operation cleaner and free from winding contamination. The metallic seals have been used for final sealing of the cooler for reducing the leak rates to minimum and more importantly for obviating the need for welding. The IDCA cryocooler prototype developed having a cooling capacity of 0.5W@80K with steady state power input of less than 10 W is shown in Fig. 3.

Figure 3. IDCA cryocooler prototype developed at SSPL.

3.1.1 Brushless DC Motor

One of the critical technologies in the development of cryocooler is the development of an efficient brushless DC (BLDC) motor. It is the crucial component of the cryocooler system and to a large extent the performance of the system depends on this esp. when it comes to high efficiency and power savings in the battlefield, where the later is limited. A specially designed BLDC motor with a compact on-board integrated electronics[17] has been developed to suit the desired physical and other characteristics governing the system performance. The inbuilt demand control is able to regulate the target space temperature within ±1 K. The motor is equipped with advance features like standby, shut-down and cool-down indicator modes. The motor delivers a maximum power of 20 W with efficiency close to 75 per cent even at the highest of working speeds.

3.2 Thermodynamic Analysis

The Stirling cooler basically works on the principle of Stirling cycle. It conceptually works by employing a pump to cyclically press the working fluid and passing it back and forth between the hot and cold regions across a regenerative heat exchanger. The pressure-volume (PV) and temperature-entropy (TS) diagrams pertaining to ideal Stirling cycle are shown in Fig. 4. The compression (1-2) and expansion processes (3-4) occurs as most efficient isothermal processes at temperatures T_c and T_e respectively, where as the regenerative cooling (2-3) and heating (4-1) of the working fluid is achieved as constant volume processes. The performance and cooling capacity of the Stirling cycle coolers depends on various parameters including the dead volume ratio, swept volume ratio, the phase angle and the temperature ratio, etc[4].

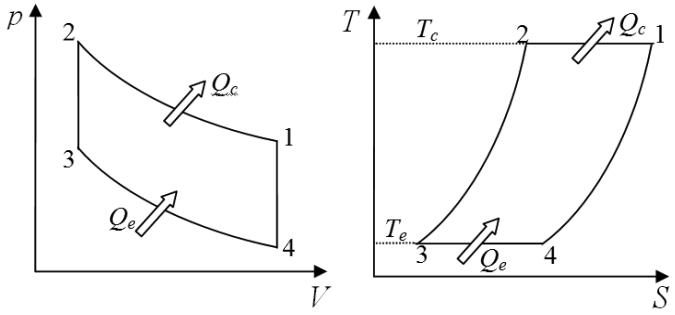

Figure 4. Ideal Stirling cycle: Pressure-volume diagram and Temperature-entropy diagram.

In the present text, the cooler has been subjected to first order thermodynamic analysis with sinusoidal motions without considering losses for performance approximations. The instantaneous volume, V_e, of expansion space can be expressed as a function of crank angle ϕ, and expansion space swept volume, V_E, and is given by

$$V_e = \frac{1}{2} V_E (1 + \cos\phi) \tag{1}$$

If the phase lag between the piston and displacer is α, then volume variations of compression space is defined as

$$V_c = \frac{1}{2} \kappa V_E (1 + \cos(\phi - \alpha)) \tag{2}$$

where k is the ratio of swept volumes, and is given by V_C/V_E. where Vc is compression space swept volume.

The cyclic cold production or the heat extracted from the expansion space Q_e is a function of V_E, mean charge pressure p_{mean}, intermediate parameters θ and δ, and is given as follows[8]:

$$Q_e = \frac{V_E \cdot p_{mean} . \delta . \pi . \sin\theta}{[\sqrt{(1-\delta^2)} + 1]} \tag{3}$$

where the parameter θ and δ are functions of dead volume ratio X, κ and α, and can be calculated as

$$\theta = \tan^{-1} \frac{\kappa . \sin\alpha}{\tau + \kappa . \cos\alpha} \tag{4}$$

Here the term τ is the temperature ratio and is defined as T_c/T_e and

$$\delta = \frac{\sqrt{\tau^2 + \kappa^2 + 2.\tau.\kappa + 2S}}{\tau + \kappa + 2S} \tag{5}$$

In above equation the term S is the reduced dead volume which is defined as

$$S = \frac{2X\tau}{\tau + 1} \tag{6}$$

where X is the dead volume ratio and can be defined as V_D/V_E; V_D being the total of all the non-swept volumes. Further the instantaneous pressure, p, is a function of maximum pressure, $p_{\max}$, and is calculated as follows.

$$p = \frac{p_{\max}(1-\delta)}{[1 + \delta.\cos(\phi - \theta)]} \tag{7}$$

where the maximum charge pressure, $p_{\max}$, is given by

$$p_{\max} = p_{mean} \sqrt{\frac{1+\delta}{1-\delta}} \tag{8}$$

Moreover considering the combined swept volume V_T and by using Eqns (3), (7), and (8), a term cyclic dimensionless heat extracted, $Q_e^* = \frac{Q_e}{p_{\max} . V_T}$, may be defined as follows

$$Q_e^* = \frac{\pi(1-\delta)^{1/2} . \delta . \sin\theta}{(1+\kappa).(1+\delta)^{1/2} . [1 + (1-\delta^2)^{1/2}]} \tag{9}$$

The work done on the system, W, may be evaluated from the following

$$W = Q_c - Q_e = (\tau - 1) . Q_e \tag{10}$$

where the heat of compression or the heat rejected by the system, Q_c, is given as

$$Q_c = \tau . Q_e \tag{11}$$

Then the ideal Coefficient of Performance COP_{ideal} is give by:

$$COP_{ideal} = \frac{Q_e}{W} = \frac{1}{\tau - 1} = \frac{T_c}{T_c - T_e} \tag{12}$$

Likewise Eqn. (9), a term dimensionless cyclic work input W^* may be defined using Eqn. (10) and can be written as follows.

$$W^* = (\tau - 1).Q_e^* \tag{13}$$

Now from Eqns. (9) and (13) the effect of various governing parameters on cooler performance can be analyzed in dimensionless terms.

3.2.1 Sample Calculations

Numerical computations have been performed for analyzing the effect of various design parameters on coolers performance, using the parameters and related material property data given in Appendix. The data pertains to the IDCA cryocooler prototype under development. Figures 5(a) and 5(b) shows the dimensionless heat extraction and work done per cycle based on variation of α and κ respectively for different dead volume ratios. The dead volume V_D considered is the total of non-swept volumes excluding the regenerator dead volume. The optimum of the heat extraction exists where the phase angle α is near to the 100° mark, and interestingly as the dead volume ratio increases the cyclic heat extraction decreases with a shift of phase angle towards the 90° mark. As can also be observed, heat extraction varies by only ±10% when the phase angle is in the range of 60° to 110°. So the advantage of manufacturing ease of making the 90° arrangement overweighs the sacrificing a minuscule of the cooling power especially where the dead volume ratios may have larger values due to the inherent ducting arrangements. Further, it can be clearly observed from Fig. 5(b) that this optimum exists when the swept volume ratio κ is near to 3 for the present case.

It is clear that the above results help a designer in choosing the optimized values of various parameters for a preliminary design, but numerous other factors govern the actual attainable cold production that will become more evident in next section.

3.3 Loss Evaluation of System

In the previous section, we did not consider the losses and it was assumed that the system is ideal. However, in real system there are losses due to the non-ideality that persists inherently in the system. The evaluation of losses is necessary for predicting the actual cooling capacity and also from the point of view of impact of these losses in deciding the configuration and materials of different components of the system. These losses have the detrimental effect of reducing the refrigeration produced. Now consider the actual coefficient of performance of the cryocooler, COP_{actual}, which may be defined as follows.

$$COP_{actual} = \frac{Q}{P} \tag{14}$$

where Q is the actual cooling capacity of real system and P is the corresponding actual power input. The term Carnot efficiency gives the numerical value of the deviation from the most ideal behavior, and is defined as[8]

$$\eta_{Carnot} = \frac{COP_{actual}}{COP_{ideal}} \tag{15}$$

Considering the most ideal behavior of the cooler and using Eqn. (12), for cooler working in the temperature range of T_c=300K and T_e=80K the COP_{ideal} comes out to be 0.36. Now, consider the actual typical miniature cooler, as is our case, with cooling capacity of 0.5W and power input of 15W, COP_{actual} value is around 0.033, and the Carnot efficiency as calculated from Eqn. (15) is barely 0.092, and a large amount of the power is consumed in overcoming the losses. Hence, a system level loss assessment is necessary for producing efficient coolers. Broadly, the losses can be divided into the following two categories[18].

a. Losses that consume the fraction of input power available for the refrigeration like joule heating in coil windings and irreversible compression etc., and are mostly related to the compressor part.

b. Losses that consume a part of refrigeration directly, and are related to the expander side.

In the present study the second category of losses have been considered, since these have direct impact on the coolers performance and can be controlled with less effort as compared to the other losses.

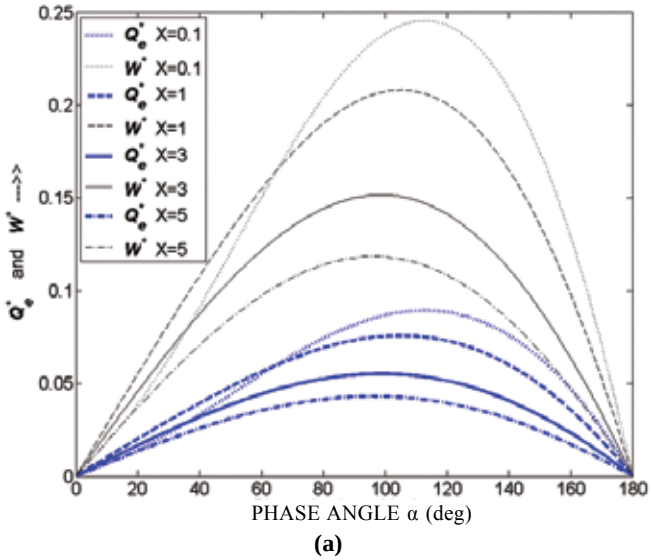

(a)

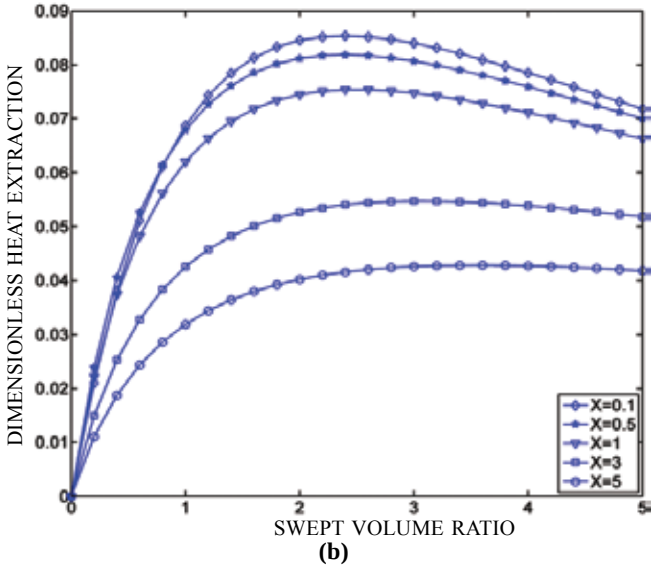

(b)

Figure 5. Effect of design parameters on dimensionless heat extraction and/or work done for different dead volume ratios X: (a) Phase angle α (b) Swept volume ratio κ.

The net refrigeration available at cold end for cooling the actual load can be calculated from the following.

$$Q_{net} = Q_e - (\underbrace{Q_{ief} + Q_{\Delta p_f} + Q_{rt} + Q_{cmg}}_{\text{Regenerator Losses}} + Q_{shtl} + Q_{dewar}) \quad (16)$$

where Q_{net} is actual net refrigeration available for cooling the application load, i.e. the detector array, Q_e is maximum refrigeration available in ideal Stirling cycle as given in Eqn. (3), the bracketed values are the sum of all the losses in which Q_{ief} is the loss due to thermal ineffectiveness of regenerator, $Q_{\Delta p_f}$ is the loss due to frictional pressure drop Q_{rt} is conduction loss associated with regenerator tube, Q_{cmg} is longitudinal conduction loss of regenerator matrix whereas Q_{shtl} and Q_{cf} are the shuttle heat transfer loss and dewar (conduction and radiation) losses respectively. The following sub-sections cover the analysis of these losses, with a special emphasis given to the regenerator design optimization as an outcome of this analysis.

3.3.1 Regenerator Losses and Design Optimization

As can be seen in Eqn. (16), a large part of the losses is solely attributed to the regenerator component. Hence the regenerator in Stirling cryocooler assumes great importance. As compared to the larger units it becomes even more crucial in case of small capacity coolers where most of the cooling effort of the machine goes in overcoming the losses arising out of regenerator. The major part of the actual refrigeration available to cool a thermal load is consumed by the thermal and flow losses associated with regenerator.

The main function of the regenerator is to store maximum energy with minimum of the losses. In this context, a term regenerator efficiency is defined which is a function of total energy losses and the maximum heat storage in regenerator[19]. It gives a fair estimate of regenerator performance by accounting for the penalty incurred in attempt to store energy. In the present study the attempt has been made to optimize the regenerator design by maximizing the regenerator efficiency. Here, the design problem is basically to select the geometry of regenerator, which includes the wire-mesh specifications and the length of regenerator matrix, to give maximum efficiency.

3.3.1.1 Regenerator Ineffectiveness Loss

Because of the ineffectiveness of the regenerator, the temperature of the gas leaving the cold end of the regenerator is somewhat higher than the matrix temperature or some of the cooling effect is lost in cooling the gas to source temperature. This loss is called the regenerator ineffectiveness loss which is given as:

$$Q_{ief} = \dot{m}.C_p.(T_c - T_e).(1-\varepsilon) \quad (17)$$

where $\dot{m}$ being the mass flow rate and C_p is the specific heat of fluid. The regenerator effectiveness is a function of many parameters which includes mass and material of matrix, frequency, number of heat transfer units *Ntu*, and heat capacity ratios of material and gas. The effectiveness is given by the following equation[15].

$$\varepsilon = \frac{Crs}{Ntu(1+Crs)^2}[(\exp(-Ntu)\int_0^{\eta - Ntu/Crs}[1+2Crs+(1+Crs)(\eta - \frac{Ntu}{Crs} - z) + \ldots$$

$$\ldots Crs^2.\exp\{-(1+Crs)(\eta - \frac{Ntu}{Crs} - z)\}]\exp(-z).I_0.(2.\sqrt{Ntu.z}).dz$$

$$+ \frac{Ntu(1+Crs)^2}{Crs} - (1+Crs)\eta - Crs[1-\exp\{-(1+Crs)\eta\})]$$

$$\ldots. \text{For } (\eta > \frac{Ntu}{Crs})$$

$$= \frac{Crs}{Ntu(1+Crs)^2}\left[\frac{Ntu(1+Crs)^2}{Crs} - (1+Crs)\eta - Crs[1-\exp\{-(1+Crs)\eta\})]\right]$$

$$\ldots. \text{For } (\eta \le \frac{Ntu}{Crs}) \quad (18)$$

where

$$Ntu = \frac{h_m.A}{\dot{m}.C_p}\ ,\ \eta = \frac{Ntu}{Cr}\ ,\ Crs = \frac{M.C_m}{l_r.A_f.\rho_0.C_p}\ ,\ Cr = \frac{M.C_m}{\dot{m}.C_p.t}$$

where *Cr* and *Crs* are the heat capacity ratios of matrix material to the fluid flowing through the matrix and matrix material to fluid in void volume respectively. Further, the function $(2.\sqrt{Ntu.z})$ is modified Bessel function of the first kind of the order zero. The heat transfer coefficient is calculated as

$$h = \frac{k_f.N_{ud}}{d_m} \quad (19)$$

where $N_{ud} = 0.42\,\mathrm{R}_{ed}^{0.56}$ where N_{ud} is Nusselt number for wire screen and Reynolds number is given as

$$\mathrm{R}_{ed} = \frac{d_m u}{\upsilon} \quad (20)$$

3.3.1.2 Pressure Drop Loss

The pressure drop loss caused by the frictional flow across the regenerator matrix which reduces the magnitude of the pressure available for expansion thereby reducing the area of expansion space *p-v* diagram and the gross refrigeration produced. The pressure drop is expressed as[15]

$$\nabla p_f = f.\rho.u^2.n/2 \quad (21)$$

The flow friction factor *f* is defined as

$$f = \frac{33.6}{\mathrm{Re}_l} + 0.337 \quad (22)$$

where Re_l is Reynolds number can be evaluated as

$$\mathrm{Re}_l = \frac{l_m.u}{\upsilon} \quad (23)$$

The pressure drop loss can be calculated from the following equation[12]:

$$Q_{\Delta p_f} = \frac{Q_e.\Delta p_f}{Pa} \quad (24)$$

where *Pa* is pressure amplitude of the cycle, which is given in terms of compression ratio as

$$Pa = P_{mean}\frac{r-1}{r+1} \quad (25)$$

3.3.1.3 Longitudinal Conduction Loss

Longitudinal conduction through regenerator tube is given as :

$$Q_{rt} = \frac{k_m.A_t.(T_c - T_e)}{l_r} \quad (26)$$

whereas the longitudinal conduction through matrix and gas can be calculated from[19]:

$$Q_{cmg} = \frac{k_{eff}.A_{eff}.(T_c - T_e)}{l_r} \quad (27)$$

where k_{eff} is the void space effective thermal conductivity of matrix and gas and is given as

$$k_{eff} = k_f \cdot \frac{(1 + k_m / k_f) - (1 - \phi).(1 - k_m / k_f)}{(1 + k_m / k_f) + (1 - \phi).(1 - k_m / k_f)} \quad (28)$$

And A_{eff} is the effective conduction area which may be written as:

$A_{eff} = A_r(1 - \phi)$; where ϕ is the porosity of wire-mesh.

3.3.1.4 Regenerator Efficiency

The regenerator efficiency from its definition may be written as

$$\Psi = 1 - \frac{Q_t}{Q_{st}} \quad (29)$$

where Q_t is the total of regenerator losses as explained above and Q_{st} is the total heat stored in matrix which is

$$Q_{st} = \dot{m}.C_p.(T_c - T_e).\varepsilon \quad (30)$$

3.3.2 Shuttle Heat Transfer and Dewar Losses

This loss is a form of motional convective heat transfer which occurs when the displacer with an axial temperature gradient reciprocates inside the cylinder of cold-finger with a similar axial temperature gradient and causes an extra heat transfer from the high to the low temperature region in addition to the wall conduction[20]. This loss is calculated using the following equation as suggested in ref.[21]

$$Q_{shtl} = \frac{k_f.\pi.d_r.s^2.(T_c - T_e)}{(5.4).C.l_r} \quad (31)$$

where *s* is the stroke length and *C* is the radial clearance.

Dewar losses constitute the conduction and radiation in dewar vessel including the cold-finger. The conduction losses are those occurring through the wall of the cold-finger due to the thermal gradient that prevails between the two ends The radiation loss comes from the radiation heat exchanged between the dewar vessel inner wall and the external surface of the cold-finger tube.

3.3.3 Results

The computation of losses and regenerator design optimization has been done considering the IDCA cooler data given in appendix. For this purpose a code has been written in MATLAB. The flow chart of the methodology followed is shown in Fig. 6. Various wire-mesh sizes ranging from 100 to 500 mesh number have been selected for the analysis. Mesh-sizes below 100 are not considered due to very low values of effectiveness. Stainless steel wire-mesh is chosen due to its favorable heat capacity and thermal properties in the temperature range of cooler operation[22,23]. Regenerator losses and efficiency is then calculated for each mesh-size by computing the regenerator effectiveness from Eqn. (18), which also considers the heat capacities and void volume effects. Then the optimum mesh size and length is chosen based on maximum efficiency.

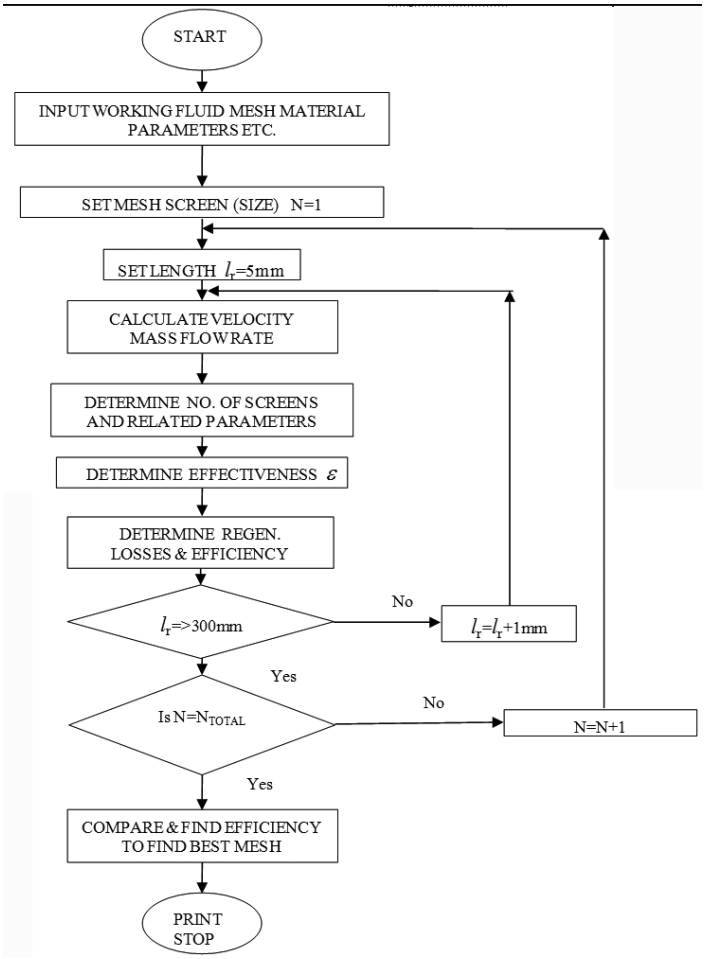

Figure 6. Regenerator design optimization procedure.

Various regenerator losses are plotted in Fig. 7(a) for a 400 size mesh as a function of regenerator length. It can be observed that regenerator ineffectiveness loss and other longitudinal conduction losses decreases with increasing length while the flow losses due to drop in pressure increases. Regenerator efficiency is plotted in Fig. 7(b), where the mesh sizes 300 and 400 are the best choices for a length zone of 35-45 mm. The heat balance for IDCA cryocooler has been presented in Table 1.

3.4 Experimental Results

A total of three prototypes were fabricated, assembled and tested for performance. Test results are summarised in Table 2.

Cooler was said to be failure if it does not meet the following conditions.

- Maximum input power < 20 W

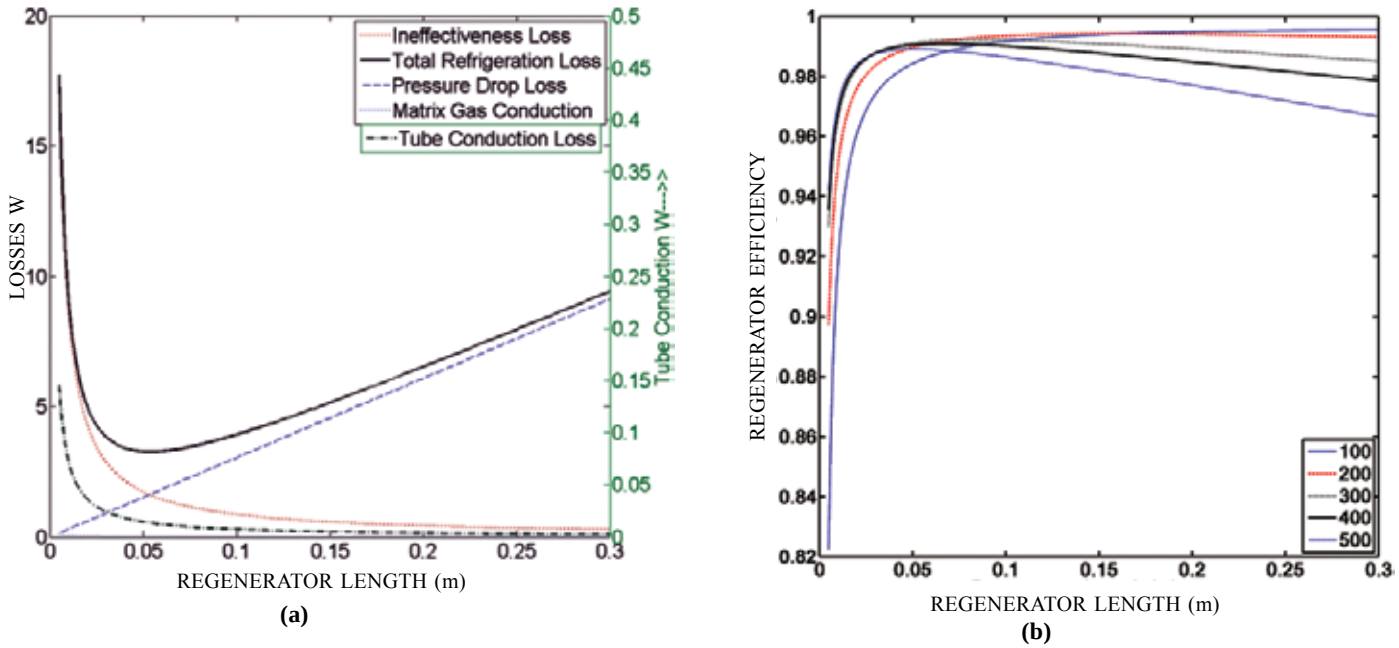

Figure 7. (a) Regenerator losses for a 400 mesh size (b) Regenerator efficiency for different mesh sizes.

Table 1. Heat balance sheet for IDCA cryocooler

Regenerator ineffectiveness loss, Q_{ief}	2.26 W
Pressure drop loss, $Q_{\Delta pf}$	1.15 W
Regenerator longitudinal conduction, $Q_{rt}+Q_{cmg}$	0.04 W
Shuttle heat loss, Q_{shtl}	0.33 W
Dewar heat load, Q_{dewar}	0.32 W
Total losses (A)	4.10 W
Ideal heat extracted Q_e (B)	5.07 W
Available refrigeration Q_{net} (C=B-A)	0.97 W
Actual cooling requirement for detector (D)	0.20 W
Losses unaccounted for (C-D)	0.77 W

- Cold tip temperature < 80 K
- Cool down time < 8-9 min depending upon ambient temp.

All the above parameters were monitored through a data acquisition (DAQ) system developed 'in-house'. Typical thermal performance test results are shown in Fig. 8 as a screen-shot of DAQ system, depicting the cold-tip temperature and the power input with time. It is evident from the results that the prototypes met the above conditions. The prototype PS-I was integrated with the detector-dewar assembly, primarily to determine the heat load capacity and size compatibility whereas the prototypes PD-01 and PD-02 were tested in dummy vacuum jacket of known heat load. The prototype PD-02 has operated for 330 cumulative hrs intermittently, but when put on continuous run it failed after 59 h. Similarly PS-I has run for 120 cumulative hrs, but failed after a continuous run of 19 h. Cause of failure is attributed to the poor quality of main housing bearing. All out efforts are in progress to find good quality bearings to enhance the lifetime and reliability of the cryocooler.

Table 2. Experimental test results of IDCA cryocooler

Cooler type	Cold tip temp (K)	Max. power (W)	Regulated power (W)	Cool down time (Min)	Ambient temp (°C)	Heat load (mW)	Status	Continuous running (hrs)	Failure mode	Remarks
PD-01	70.3	15 - 16	--	6 - 7	25	350	operating	50	None	To test the endurance of regenerators
PD-02	77	15 - 16	--	6 - 7	20	350	failed	59	Bearing failure	Hard chromium coating on piston
PS-I	80	15	8	7	15	285	failed	20	Bearing failure	Ti- Nitride coating on piston

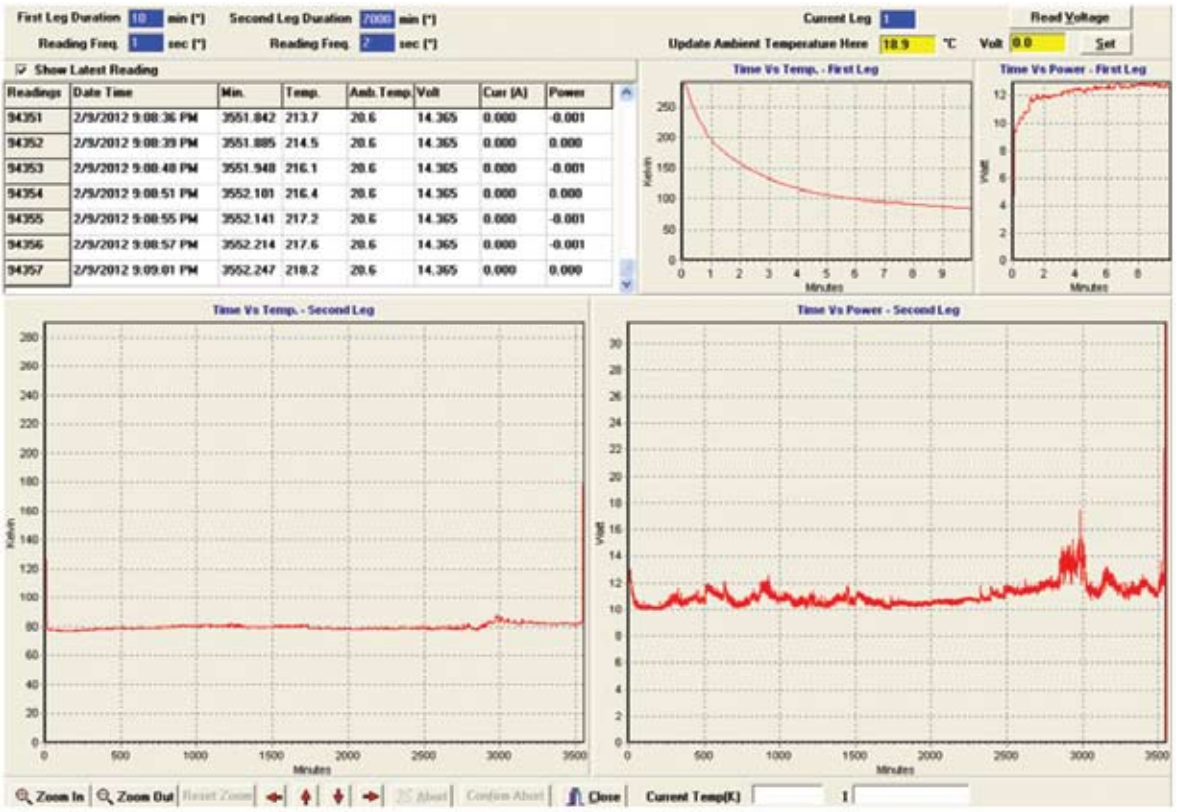

Figure 8. DAQ screen-shot of a typical performance run.

4. CONCLUSION

In this paper a brief review of the activities related to the development of miniature Stirling cryocoolers especially suited to IR sensor cooling applications has been presented. The technology for linear split and rotary integral coolers have been explained in due details. Thermodynamic analysis including the loss analysis has been presented from design point of view with a special emphasis on regenerator design optimization. The theoretical as well as the relevant experimental results have been presented and discussed.

Prototypes of both split and integral types have been tested in laboratory and also integrated with the thermal sight successfully. Optimization efforts to enhance the reliability and life time are still in progress. We expect to achieve these goals by carrying out further design modifications and will be in a position to predict MTTF of the coolers once produced in sufficient numbers. The cryocooler will also be subjected to environmental testing to make it usable in field application in future.

ACKNOWLEDGEMENT

Authors are grateful to Director, Solid State Physics Laboratory (SSPL) for his constant support and encouragement during the course of this work. We are grateful to Mr Saket Mital, Mr K. Upadhayay and Mr Ramesh Chandra for their help in conducting experiments and documentation work. Thanks are also due to the SSPL workshop staff for fabrication of components.

REFERENCES

1. Richard, D. Hudson. Jr. Infrared system engineering. John Wiley & Sons, New York, 1969. pp.642
2. Breckenridge Jr, R.W. Cryogenic coolers for IR systems. *Optical Engineering*, 1975, **14**(1), 140-157.
3. Walker, G.; Fauvel, R. & Reader, G. Miniature refrigerators for cryogenic sensors and cold electronics. *Cryogenics,* 1989, **29**(8), 841-845.
4. Walker, G. Miniature refrigerators for cryogenic sensors and cold electronics. Clarendon Press, Oxford New York, 1989. 204 p.
5. Stolfi, F. & De Jonge, A. K. Stirling cryogenerators with linear drive. *Philips Tech. Rev.* , 1985, **42**(1) , 1-10.
6. De Jonge, A.K. & Sereny, A. Analysis and optimisation of linear motor for compressor of a cryogenic refrigerator. *In* Advances in cryogenic engineering, 1982, **27**, pp. 631-640.
7. Koh, D.Y.; Hong, Y. J.; Park, S.J.; Kim, H.B. & Lee, K.S. A study on the linear compressor characteristics of the Stirling cryocooler. *Cryogenics*, 2002, **42**(6), 427-432.
8. Walker, G. Cryocoolers Part 1: Fundamentals. Plenum Press, New York and London, 1983. 364 p.
9. Tailor, P.R. & Narayankhedkar, K.G. Thermodynamic analysis of the Stirling cycle. *Cryogenics*, 1988, **28**(1), 36-45.
10. Orlowska, A.H. & Davey, G.. Measurement of losses in a Stirling cycle cooler. *Cryogenics*, 1987, **27**(11), 645-651.
11. Reed, J.S.; Davey, G.; Dadd, M.W. & Bailey, P.B. Compression losses in cryocoolers. *Cryocoolers,* 2005,

13, 209-214.
12. Yang, X. & Chung, J. N. Size effects on miniature Stirling cycle cryocoolers. *Cryogenics*, 2005, **45**(8), 537-545.
13. Chhatwal, H.L.; Goswami, T.R., & Dewakar, R.K. Miniature linear motor driven integral type Stirling cooler for laboratory use. *Indian J. Pure Appl. phys.*, 1992, **30**(12), 771-772.
14. Chhatwal, H.L.; Goswami, T.R. & Dewakar, R.K. Prototype miniature split Stirling cryo-cooler. *Indian J. Pure Appl. phys.*, 1993, **31**(11), 794-797.
15. Miyabe, H.; Hamaguchi, K. & Takahashi, K. An approach to the design of Stirling engine regenerator matrix using packs of wire gauzes. *In* Proceeding IEEE, IECEC, 1982, **17,** pp. 1839-1844.
16. Hanselman, Duane C. Brushless permanent-magnet motor design. McGraw-Hill, New York, 1994, 392p.
17. Ruehlich, I.; Korf, H. & Schellenberger, G. Advanced control electronics for Stirling cryocoolers. *In* Proceedings of SPIE, 2002, **4820**, pp. 15-25.
18. Thirumaleshwar, M. & Subramanyam, S. V. Heat balance analysis of single stage Gifford-McMahon cycle cryorefrigerator. *Cryogenics*, 1986, **26**(3), 189-195.
19. Pande, G.V. & Narayanamurthy, H. Design studies for stirling cycle cooler regenerator. *J. Spacecr. Techno.*, 1995, **5**(1), 57-63.
20. Chang, H. M.; Park, D. J. & Jeong, S. Effect of gap flow on shuttle heat transfer. *Cryogenics*, 2000, **40**(3), 159-166.
21. Zimmerman, F.J. & Longsworth, R.C. Shuttle heat transfer. *In* Advances in cryogenic engineering. 1970, **16**, pp. 342-351.
22. Andeen, B.R. Heat capacity and geometry impacts on regenerator performance. *In* Advances in Cryogenic Engineering. 1982, **27**, pp. 611-619
23. De Waele, A.T.A.M. Finite heat-capacity effects in regenerators. *Cryogenics*, 2012, **52**(1), 1-7.

CONTRIBUTORS

Mr Manmohan Singh obtained his M.E (Thermal Engineering) from Delhi college of Engg., Delhi University. Presently, he is working as Head, Cryogenics Group, SSPL Delhi. His research interest includes manufacturing technology and Stirling cryocoolers.

Mr Sunil Suchdev received his AMIE degree in Mech. Engg. He is working as Scientist in Cryocooler Group and his current interests include the development of cryocooler systems for defence applications.

Mr Mukesh Sadana received his Masters degree from IIT, Delhi in 2009. He is working as Scientist and his current interests include the development of cryocooler systems and dynamics of machines.

Mr Gaurav Pratap received his BTech from K.N.I.T, Sultanpur in 2006. He is working as Scientist and his current interests include the development of cryocooler systems for defence applications.

APPENDIX

Cryocooler parameters	
Nominal speed	4000 rpm
Stroke length	2 mm
Dead volume ratio	2.87
Swept volume ratio	3.48
Phase angle	90 ^{o}
Ambient temperature	300 K
Cold-tip temperature	80 K
Average temperature (T)	190 K
Charge pressure	25 bar
Piston diameter	14 mm

Working fluid - Helium properties	
Density of Helium at T	6.33 kg/m^3
Specific heat of Helium at T (above)	5.19 kJ/kg.K
Thermal conductivity of Helium at T	0.11 W/m.K
Dynamic viscosity of Helium at T	1.46E-05 N.s/m^2

SS Wire mesh parameters	
Density	7900 kg/m^3
Specific heat	0.4 kJ/kg.K
Thermal conductivity	12.6 W/m.K
Mesh size no.	400

Regenerator parameters	
Regenerator tube thickness	0.5 mm
Regenerator internal diameter	6.5 mm
Thermal conductivity of regen. tube	0.3 W/m.K
Regenerator length	38 mm
Regen. radial clearance	35 µm
Capacity ratio *Crs*	40
Capacity ratio *Cr*	33